Published in final edited form as:
Mol Imaging. 2010 August ; 9(4): 201–210.

Ferritin Overexpression for Noninvasive MRI-Based Tracking of Stem Cells Transplanted into the Heart

Anna V. Naumova, Ph.D.[1,3], **Hans Reinecke, Ph.D.**[2,3], **Vasily Yarnykh, Ph.D.**[1,3], **Jennifer Deem**[2,3], **Chun Yuan, Ph.D.**[1,3,4], and **Charles E. Murry, M.D., Ph.D.**[2,3,4]

[1]Department of Radiology, University of Washington, Seattle, WA

[2]Department of Pathology, University of Washington, Seattle, WA

[3]Center for Cardiovascular Biology, Institute for Stem Cell and Regenerative Medicine, Seattle, WA

[4]Department of Bioengineering, University of Washington, Seattle, WA

Abstract

An unmet need in cardiac cell therapy is a non-invasive imaging technique capable of tracking changes in graft size over time and to monitor cell dynamics such as replication and death, factors to which commonly used paramagnetic nanoparticles are insensitive. Our goal was to explore if overexpression of ferritin, a non-toxic iron-binding protein, can be used for non-invasive magnetic resonance imaging (MRI) of cells transplanted into the infarcted heart.

Mouse skeletal myoblasts (C2C12 cells) were engineered to overexpress ferritin. Ferritin overexpression did not interfere with cell viability, proliferation or differentiation into multinucleated myotubes. Ferritin overexpression caused 25% decrease of T2 relaxation time *in vitro*, compared to wild-type cells. Transgenic grafts were detected *in vivo* 3 weeks after transplantation into infarcted hearts of syngeneic mice as areas of hypointensity caused by iron accumulation in overexpressed ferritin complexes. Graft size evaluation by MRI correlated tighly with histological measurements (R^2=0.8).

Our studies demonstrated the feasibility of ferritin overexpression in mouse skeletal myoblasts and the successful detection of transgenic cells by MRI *in vitro* and *in vivo* after transplantation into the infarcted mouse heart. These experiments lay the groundwork to use the MRI gene reporter ferritin to track stem cells transplanted to the heart.

Keywords

Myocardial infarction; MRI; ferritin; gene reporter; cell transplantation

Address for Correspondence: Anna V. Naumova, PhD., University of Washington, 815 Mercer Street, Brotman Building, Room, 124, Seattle WA, 98109. Phone 206-897-1310. Fax: 206-616-9354. nav@uw.edu.

DISCLOSURES

We have no conflicts of interest to disclose.

INTRODUCTION

Stem cells have the ability to differentiate into a diverse range of specialized cell types, giving them a potential to dramatically change the treatment of human disease. Heart failure due to myocardial infarction is a major cause of death worldwide. Cell transplantation using derivatives of adult or pluripotent stem cells is widely investigated as a promising therapeutic approach for heart failure [1–3]. Current methods of studying stem cell engraftment rely heavily on postmortem histological sampling. There is a lack of suitable imaging technology for serial non-invasive tracking of therapeutic cell after their engraftment. Stem cell labeling with superparamagnetic iron oxide nanoparticles (SPIOs) allows labeled cells to be detected by magnetic resonance imaging (MRI) and is commonly used to track stem cell engraftment [4, 5]. However, the MRI signal hypointensity caused by those particles does not reflect the actual cell number after several rounds of cell division due to particle dilution. In addition, MRI signal from iron oxide nanoparticles does not represent live cells; particles released from dead cells can be phagocytosed by host cells, thereby misleading MRI tracking [6, 7]. Both of these reasons preclude monitoring of long-term stem cell engraftment.

Molecular tagging of graft cells by overexpression of non-toxic MRI-detectable probes, such as the iron-binding protein, ferritin, is an alternative approach that may solve the cell tracking problem [8, 9]. The use of reporter genes for MRI-based cell tracking offers two important advantages over particle-based techniques: 1) gene expression is correlated much more tightly with cell viability than is particle retention; and 2) when integrated into the genome, transgene based reporters are much less susceptible to signal loss through cell division and therefore are uniquely suited for longitudinal monitoring of cell transplants.

The unique structure and properties of ferritin make it valuable as an MRI reporter. Ferritin is the main intracellular iron storage protein and has a globular structure 12.0nm in diameter, accumulating significant amounts of hydrous ferric oxide iron in its core [10]. Ferritin can be considered an “endogenous nanoparticle”. The protein shell isolates iron from the cytoplasm, preventing elevation of hydroxyl radical formation [11, 12]. It has been shown that ferritin overexpression can be detected by MRI in C6 glioma tumors [8], used for *in vivo* studies in the mouse brain [9, 13] and for imaging of subcutaneous inoculation of undifferentiated mouse embryonic stem cells [14].

The potential of using ferritin overexpression for noninvasive imaging of stem cell transplanted into infarcted heart has not been explored. In this study we aimed to develop a genetically-based technique for molecular imaging of ferritin-tagged cells transplanted into infarcted rodent hearts. Our principal hypotheses for this study were: 1) ferritin overexpression is non-toxic for transduced cells, i.e. it does not affect cell viability, proliferation or differentiation; 2) ferritin overexpression in transduced cells is detectable by MRI *in vitro* and *in vivo* after transplantation into infarcted murine heart; 3) tagging of transplanted cells by ferritin permits accurate quantification of graft size in the heart.

MATERIALS AND METHODS

Ferritin Expression Vector Design

The murine ferritin heavy-chain cDNA with an HA (influenza hemagglutinin) epitope tag (HA-ferritin) was obtained from Dr. Neeman and Dr. Cohen at the Weizmann Institute, Israel [8]. BamHI and HindIII double digestion was used for identifying of HA-ferritin presence in the pGEM-T vector. HA-ferritin was released from pGEM-T vector backbone using EcoR1 restriction sites and was then ligated into the pcDNA3 vector plasmid downstream of the cytomegalus virus (CMV) promoter, thus enabling strong transgene expression and selection of stably transduced cells via neomycin (G418) resistance. DNA sequencing confirmed fidelity of the construct. Mouse C2C12 skeletal myoblasts were transfected with pcDNA3-HA-ferritin cDNA using FuGENE6 reagent and cells were cultured on gelatin-coated tissue culture dishes in growth medium (DMEM, Invitrogen) supplemented with 20% fetal bovine serum (HyClone, Logan, UT), 2 mM L-glutamine (Invitrogen) and penicillin/streptomycin. Neomycin (G418) was added to the cell culture media at 1.2mg/mL to select for stably transduced cells. G418-selected colonies were trypsinized, replated as mixed mass cultures and maintained in G418 containing growth media until use. C2C12 subclones were created by dilute plating of cells and isolation of the subclones using cloning rings.

Assessment of C2C12 Proliferation

Cell proliferation was assessed by monitoring the total number of cells plated in 6-well plates (5,000 cells per well) during one week of growth using a Beckman Coulter Counter. We compared growth of wild type and HA-ferritin C2C12 cells both with and without ferric citrate supplementation (1mM). All calculations were done in duplicates.

Assessment of C2C12 Differentiation

To assess the effect of ferritin overexpression on differentiation of C2C12 cells into multinucleated myotubes, wild type and transgenic cells were subjected to a myogenic differentiation protocol where growth media is replaced by DMEM containing 5% horse serum. Cells were maintained in differentiation media for 7 days, and then fixed with ice-cold methanol. Myosin heavy chain was visualized using monoclonal anti-fast skeletal myosin heavy chain antibody MY32 (1:400 dilution).

Western Blot Analysis

To assess trangene protein expression, $5x10^5$ HA-ferritin and wild type (control) C2C12 cells were lysed, homogenized, and electrophoresed in 12% polyacrylamide gel (30 μg/lane) using technique described in [15]. Membranes were incubated overnight (4°C) with either anti-HA mouse non-conjugated monoclonal antibody (1:1000; Covance, Inc., Emeryville, CA), or rabbit non-conjugated monoclonal anti-ferritin antibody (1:2000; Abcam Ltd., Cambridge, MA). Identical blots were prepared and incubated with a mouse non-conjugated monoclonal antibody against β-tubulin (1:400; Sigma, St.Louis, MI) as a control for protein loading. Either, horseradish peroxidase–conjugated goat anti-rabbit antibody (ferritin

detection), sheep anti-mouse antibody (HA-tag detection), or rat anti-mouse antibody (β-tubulin detection), all 1:5000 in TBS-T were used as secondary antibodies.

Iron Detection by Prussian Blue Staining

Prussian Blue staining was used to confirm iron accumulation in the cytoplasm. C2C12 cells plated in 6-well plates were washed twice with PBS, and then fixed with 2% paraformaldehyde for 10 minutes. Equal amounts of 20% hydrochloric acid and 10% potassium ferrocyanide solution were mixed, and then added to 6-well plates for 20 minutes. Nuclear fast red was used as a counterstain. In this assay, the presence of iron was indicated by a bright blue color in a granular cytoplasmic distribution.

Measurements of T2 Relaxation Time by MRI in Cell Samples

To test the capability of MRI to detect ferritin overexpression, T2 relaxation times were measured in suspensions of wild type (WT) and ferritin-transduced C2C12 cells cultured with and without ferric citrate supplementation (1 mM for 48 hours). For *in vitro* imaging, WT and transgenic C2C12 cells were grown in maxi dishes, washed with PBS to remove excess of iron, then trypsinized and imaged alive in Eppendorf tubes. 300μl of 2% agarose were added to the Eppendorf tubes first, then, after the agarose had cooled off, cells were added in 1ml of media ($6x10^7$ per tube). Cells settled down in Eppendorf tubes and formed a loose pellet on top of the agarose. T2 measurements were obtained from a single slice aligned through the center of the live cell pellets on a 3T Achieva Philips scanner with a custom-built solenoid coil. A multiple spin-echo pulse sequence with 32 equally spaced echoes (10ms echo spacing) and repetition time TR=5000 ms was used. A T2 map was reconstructed from variable TE images by pixel-based fit of a single-exponential signal equation: $I = I_0 e^{-TE/T2}$, where I was the signal intensity, proton density (I_0) and T2 were fitted parameters. T2 values were measured from the T2 map in homogenous regions-of-interest placed in the center of each sample.

Myocardial Infarction in C3H mice and C2C12 injection

All animal procedures described were approved by the University of Washington (Seattle, WA) Institutional Animal Care and Use Committee and performed in accordance with federal guidelines. The C2C12 myoblast line was originally derived from the C3H mouse [16] and, therefore, we chose this mouse strain as recipient to minimize immunological rejection of engrafted cells. Mice were anesthetized by intraperitoneal injection of 2.5% Avertin (Phoenix Pharmaceuticals; 0.02–0.026ml/g), intubated and mechanically ventilated with supplemental oxygen and 3 cm H_2O of positive end-expiratory pressure (PEEP). The heart was exposed via an open thoracotomy and subjected to myocardial injury by permanent ligation of the left anterior descending artery by 8-0 Prolene suture. After verification that coronary occlusion had occurred (blanching of the tissue distal to the suture), C2C12 cells suspended in 7μl of serum/antibiotics-free medium were directly injected into the border of infarcted region of the left ventricle using a 30-gauge needle. 150,000 or 500,000 cells were injected per animal in two injection sites (3.5μl per site). Six C3H mice received 150,000 cells ferritin-tagged cells, 6 animals received 500,000 ferritin-

tagged cells, and 4 mice received WT C2C12. The chest was then closed aseptically, and animal recovery from surgery was monitored in a heated chamber.

In Vivo and *Ex Vivo* MRI of the Murine Heart

Mouse hearts were imaged on a 3T Philips Achieva clinical scanner three weeks after the surgery. Mice were anesthetized with 1.5% isoflurane in oxygen (1 liter/min) delivered through a nose cone, and placed in a solenoid mouse coil (Philips Research Laboratories, Hamburg, Germany) with built-in heating system maintaining physiological body temperature. Single-lead ECG was recorded from needle subcutaneous electrodes attached to animal's extremities and was used to trigger the MRI acquisitions using commercial software ("Small Animal Monitoring and Gating System", SA Instrument Inc., Stony Brook, NY).

Each animal was imaged alive and immediately after sacrificing by lethal dose of pentobarbital to confirm presence of the graft. This approach assured identification of hypointense MRI signals in transgenic grafts and distinguished true signal from motion and flow artifacts. *In vivo* imaging protocol included 2D ECG-gated T2*-weighted bright-blood cine turbo-field-echo (TFE) sequence (TR/TE=15/9.3ms; flip angle 15°; slice thickness 0.8mm; resolution 197x160μm), and black-blood iMSDE (improved motion sensitized driven equilibrium) prepared TFE-sequence (TR/TE=16/9.8ms; flip angle 15°; slice thickness 0.8mm, resolution 197x160μm). The advantage of iMSDE sequence is improved artifact and blood suppression [17] and, therefore, more reliable detection of engrafted cells. For graft detection *ex vivo*, a 3D multiple gradient-echo sequence (range 4.9–21.8ms, echo spacing 4.2ms); TR=61.8ms; flip angle 10°; slice thickness 0.5mm; resolution 197x120μm; two signal averages.

Histological Analysis of C2C12 Graft in Mouse Heart

After euthanisia hearts were fixed in methyl Carnoy's solution and processed for histological analysis. Five μm thick tissue sections were cut for histological staining. Skeletal muscle grafts in mouse hearts were identified using a mouse monoclonal antibody against embryonic skeletal myosin (hybridoma supernatant, 1:100, Developmental Studies Hybridoma Bank, University of Iowa). Sections were blocked with 1.5% normal goat serum in PBS and incubated for 1 hr at room temperature with the biotinylated primary antibody (Animal Research Kit, Dako). Sections were then incubated for 30 min at room temperature with HRP-conjugated streptavidin (Dako), developed with 3,3-diaminobenzidine (DAB; Sigma), and counterstained with hematoxylin (Sigma). Photographs of heart sections were taken with a QColor 3 Olimpus digital camera and a Nikon Eclipse 80i microscope.

Statistical Analysis

Correlation in graft size measurements assessed by MRI was compared with histological evaluation (embryonic skeletal myosin staining) using Pearson's correlation coefficient. Cell proliferation data were analyzed using t-test for unequal variances. Microsoft Excel and SPSS 12.0 statistical software were used for analysis.

RESULTS

Ferritin Overexpression in Skeletal Myoblasts

Mouse C2C12 myoblasts were used as a test system to develop the ferritin tagging system. An epitope-tagged version of ferritin heavy chain was stably transduced into C2C12 cells using standard plasmid-based techniques, with transcription driven by the CMV promoter (pcDNA3-HAferritin). Stable ferritin transgene overexpression was confirmed by western blot analysis using mouse monoclonal HA-antibody (Figure 1A) and rabbit monoclonal antibody to ferritin (Figure 1B). Jurkat cells and SH-SY5Y cells express high levels of ferritin and served as controls. High levels of ferritin H-chain (21 kDa) were detected in transgenic C2C12 mass culture as well as in a randomly chosen subclone, but not in WT cells (Figure 1B). Prussian Blue staining is a sensitive technique for iron detection; it confirmed significant accumulation of iron in the cytoplasm of transduced cells after iron supplementation of the media, whereas no blue cells were observed in iron-supplemented WT controls (Figures 1C, D). Thus, significant overexpression of ferritin was achieved with increased iron-storage capacity.

Effect of Ferritin Overexpression on C2C12 Viability, Proliferation and Differentiation

WT C2C12 and cells overexpressing ferritin were grown over one month in the standard C2C12 growth medium. Cell viability was evaluated with every cell passage by Trypan Blue exclusion. No differences in viability were found between wild type C2C12 and cells overexpressing ferritin. The impact of ferritin overexpression on C2C12 proliferation was assessed by standard growth curves (Figure 2A). The proliferation of the transduced myoblasts was indistinguishable from control myoblasts during 6 days of observation. We noticed that supplementation of cell media with iron citrate in high doses (1mM) inhibited proliferation of wild type C2C12 as well as proliferation of transduced cells. However, high iron concentration in the cell media was more toxic for the wild type cells than for cells overexpressing ferritin ($p<0.05$). Supplementation of cell media with low concentrations of ferric citrate (1μM) did not effect cell growth in either wild-type or transgenic cells (data not shown). To test for possible effects of ferritin overexpression on myoblast differentiation, wild type and transduced cells were switched from growth medium to differentiation medium and cultured for 7 days. Both WT C2C12 and cells overexpressing ferritin differentiated similarly and robustly into multinucleated myotubes, as assessed by immunostaining for fast skeletal myosin heavy chain (Figure 2B). In summary, ferritin overexpression did not interfere with cell viability, proliferation or differentiation in mouse skeletal myoblasts, and ferritin increased resistance to iron toxicity.

Changes in Magnetic Relaxation Properties of Transgenic Cells Overexpressing Ferritin

The ferritin overexpressing cells were readily detectable by MRI *in vitro*, yielding significant changes in T2 compared to WT cells. T2 of transgenic cells decreased by ~25% compared to non-modified control cells (Figure 3). Supplementation of growth media by ferric citrate caused additional shortening of T2 with further amplification of the difference between WT and transgenic cells. In summary, these data show that overexpression of ferritin in C2C12 cells can be detected by MRI *in vitro*.

MRI Visualization of Ferritin-tagged Grafts in the Mouse Heart *in vivo, ex vivo* and Correlation With Histology

To validate the hypothesis that ferritin overexpression is suitable as a MRI reporter for non-invasive imaging of grafted cells, we transplanted wild type and ferritin-overexpressing myoblasts into the infarcted hearts of syngeneic C3H mice. Both, wild type C2C12 and ferritin-tagged cells successfully grew in mouse hearts and formed skeletal muscle grafts (Figure 4). The presence of transgenic grafts in the infarcted mouse heart was detected by T2*-weighted MRI as areas of hypointensity caused by accumulation of iron in overexpressed ferritin complexes. Cine MRI techniques did not detect any contractile activity of the area containing skeletal muscle grafts, consistent with previous reports of their lack of electromechanical coupling [18, 19]. MRI signal void in the graft area was detected *in vivo* 3 weeks after transplantation of transgenic cells overexpressing ferritin (Figure 4A). No signal void areas were detected by MRI in wild type grafts (Figure 4C). Embryonic skeletal myosin staining confirmed the presence of skeletal muscle grafts in the left ventricle of mouse heart after transplantation of wild type C2C12 (Figure 4D) as well as ferritin-overexpressing cells (Figure 4B). Graft cells were well differentiated and contained sarcomeric structures (Figure 4E).

Reproducibility of hypointensity area appearance on bright- and black-blood images provided additional proof of the presence of ferritin-tagged grafts (Figures 5A, 5B). The areas of signal reduction were reproducible on both image types, and therefore distinguishable from flow artifacts. Our studies showed the persistence of signal void areas in the same short axis slices of the heart *in vivo* and *ex vivo* shortly after sacrificing of the mouse (Figure 5C). Increase of echo time from 4.9 ms to 21.8 ms on *ex vivo* images revealed a magnetic susceptibility effect of iron accumulation in transgenic graft. However, longer echo time compromised the signal-to-noise ratio (Figure 5, C1–C5).

The area of signal hypointensity was measured in each MR image at the short-axis plane of the heart. Graft size was assessed as a ratio of graft area to the left ventricle (LV) in each slice. Average graft-to-LV ratio in mouse hearts 3 weeks after transplantation of 150,000 cells was 9.4% (assessed by MRI) and 13.3% (by histology). Average graft-to-LV ratio after transplantation of 500,000 cells was 22.7% by MRI and 23.1% by histology. Importantly, we found strong correlation between MRI and histological measurements of the graft size with a slope of 0.79 and a correlation coefficient R^2=0.8 ($p<0.001$, Figure 5). This relationship was not significantly different from the line of unity; the p value for slope is 0.204, the p value for intercept is 0.096, suggesting lack of bias.

DISCUSSION

The present study demonstrates the feasibility of using the MRI reporter ferritin for non-invasive imaging of cardiac grafts in the mouse heart. The major findings are: 1) stable overexpression of ferritin in C2C12 mouse skeletal myoblasts is feasible; 2) ferritin overexpression does not affect cell viability, proliferation or differentiation; 3) ferritin-tagged cells are detectable by MRI *in vitro*, yielding significant changes in signal intensity compared to wild-type cells; 4) the presence of transgenic grafts in the infarcted mouse heart

can be detected by MRI as areas of hypointensity; and 5) graft size assessed by MRI correlates well with histological measurements.

Stem cell–based cellular cardiomyoplasty is a promising therapy for myocardial infarction. This strategy attempts to enhance cardiac function by repopulating the infarcted region with viable cardiomyocytes and, therefore, holds great promise for restoration of ventricular function [20]. However, low retention and survival of transplanted cells was reported [21, 22]. Therefore, development of pro-survival strategies [23, 24] as well as novel imaging techniques to study stem cell engraftmental dynamics are mandatory. Imaging-based cell-tracking methods can potentially evaluate the short-term distribution of infused cells (using iron-oxide particles) [4–7], their long-term survival and proliferation (using gene reporter approach [25]) and cardiac differentiation (using reporter genes [26]). The major challenge is to find an optimal agent that allows sufficient contrast from the host tissue and reflects changes in graft size after cell transplantion.

We propose that natural iron storage protein ferritin will be useful for noninvasive long-term monitoring of transplanted cells into the infarcted heart. It has been shown that overexpression of the ferritin H-chain induces expression of the transferrin receptor and increases iron uptake [27]. Therefore, there are natural mechanisms that shift the iron pool the into ferritin bound storage form; this restores iron homeostasis and prevents iron cytotoxicity. Recent work by Liu [14] confirmed that transgenic cells overexpressing ferritin are characterized by increase of iron content as well as by up-regulation of transferrin receptors.

In this study, we overexpressed MRI reporter ferritin in a model cell type (C2C12) and visualized the transgenic cells *in vitro* and *in vivo* after transplantation into the infarcted hearts of syngeneic C3H mice. Importantly, ferritin did not interfere with myoblast viability, proliferation or their differentiation into multinucleated myotubes (Figure 2). This is important, because an increase in free intracellular iron is known to cause production of reactive oxygen species through Harber–Weiss/Fenton reactions, resulting in lipid, protein and DNA damage [11, 12, 28]. We noticed that supplementation of cell media with ferric citrate in high doses (1mM) inhibited proliferation of WT and transduced C2C12 cells. However, exogenous iron was more toxic for wild type cells than for cells overexpressing ferritin (Figure 2A), suggesting that the transgenic cells are better able to sequester the excess iron and limit hydroxyl radical formation.

Ferritin overexpression provided sufficient MRI contrast to make transduced cells detectable *in vitro* and *in vivo* in murine hearts. Since transverse MRI relaxivity of ferritin is much higher than its longitudinal relaxivity, we were able to detect ferritin-tagged cells using T2*-weighted bright- and black-blood image sequences in a clinical 3T scanner. It has been shown that transverse relaxivity (1/T2) linearly increases with increase of field strength [29]; therefore we would expect more effective visualization of ferritin-tagged grafts in higher magnetic field strength. Similarly, visualization of ferritin-tagged grafts should be easier in large grafts in human or large animal hearts.

Our current studies with ferritin-tagged cells are encouraging; however, significant challenges lie ahead. For example, although DNA and protein degradation occur rapidly after cell death [21], there are no data as to how rapidly ferritin complexes undergo degradation after the death of transplanted cells and for how long the MRI signal from iron persists. Study by Hu [30] demonstrated that overexpression of the bacterial iron-binding protein, MagA, in 293FT cells results in their production of magnetic iron-oxide nanoparticles, similar to magnetosomes produced by magnetotactic bacteria. Cessation of MagA induction resulted in a return of iron content in 293FT cells to control values within six days, suggesting activation of iron degradation pathways. We expect that iron in overexpressed ferritin complexes would go through the similar degradation pathways after cell death; therefore dead transgenic grafts should lose their paramagnetic properties, rendering the MRI signal from ferritin complexes useful for longitudinal monitoring of viable cells.

When transplanted cells divide, any intracellular label, including iron-oxide particles and the ferritin-stored iron, would be diluted. In this regard, continuous production of ferritin in daughter cells offers a significant advantage for cell tracking by an MRI-detectable gene reporter over particle-based cell labeling method. It will be important to determine how quickly ferritin can be produced by daughter cells and how quickly ferritin complexes can bind a sufficient amount of iron from the extracellular environment to be detected MRI.

In summary, this is the first use of MRI for detection of ferritin gene expression in cardiac grafts. These data indicate that ferritin overexpression can effectively tag stem cells transplanted into the heart. Potential future applications of this technique include studying the dynamics of adult or pluripotent stem cells after transplantation.

Acknowledgments

The authors thank Michal Neeman and Batya Cohen (Weizmann Institute, Israel) for providing HA-ferritin cDNA; Kira Bendixen, Mark Saiget and Jonathan Golob for help with Western blots; Marina Fergusson and Veronica Muskheli for help with histology; Daniel Hippe for help with statistical analysis; and Jeff W.M. Bulte (Johns Hopkins University) for helpful discussion.

This work was supported by grants NIH R01 HL64387, P01 HL03174, R01 HL084642, T32 EB001650, and Mouse Metabolic Phenotyping Center Grant U54 DK076126.

References

1. Laflamme MA, Zbinden S, Epstein SE, Murry CE. Cell-based therapy for myocardial ischemia and infarction: pathophysiological mechanisms. Annu Rev Pathol. 2007; 2:307–339. [PubMed: 18039102]
2. Chien KR, Domian IJ, Parker KK. Cardiogenesis and the complex biology of regenerative cardiovascular medicine. Science. 2008; 5;322(5907):1494–1497.
3. Dimmeler S, Zeiher AM, Schneider MD. Unchain my heart: the scientific foundations of cardiac repair. J Clin Invest. 2005; 115(3):572–583. [PubMed: 15765139]
4. Bulte JW, Kraitchman DL. Monitoring cell therapy using iron oxide MR contrast agents. Curr Pharm Biotechnol. 2004; 5:567–584. [PubMed: 15579045]
5. Kraitchman DL, Tatsumi M, Gilson WD, Ishimori T, Kedziorek D, Walczak P, Segars WP, Chen HH, Fritzges D, Izbudak I, Young RG, Marcelino M, Pittenger MF, Solaiyappan M, Boston RC, Tsui BM, Wahl RL, Bulte JW. Dynamic imaging of allogeneic mesenchymal stem cells trafficking to myocardial infarction. Circulation. 2005; 112(10):1451–1461. [PubMed: 16129797]

6. Amsalem Y, Mardor Y, Feinberg MS, Landa N, Miller L, Daniels D, Ocherashvilli A, Holbova R, Yosef O, Barbash IM, Leor J. Iron-oxide labeling and outcome of transplanted mesenchymal stem cells in the infarcted myocardium. Circulation. 2007; 116(11 Suppl):I38–I45. [PubMed: 17846324]
7. Terrovitis J, Stuber M, Youssef A, Preece S, Leppo M, Kizana E, Schär M, Gerstenblith G, Weiss RG, Marbán E, Abraham MR. Magnetic resonance imaging overestimates ferumoxide-labeled stem cell survival after transplantation in the heart. Circulation. 2008; 117(12):1555–1562. [PubMed: 18332264]
8. Cohen B, Dafni H, Meir G, Harmeliny A, Neeman M. Ferritin as an Endogenous MRI Reporter for Noninvasive Imaging of Gene Expression in C6 Glioma Tumors. Neoplasia. 2005; 7(2):109–117. [PubMed: 15802016]
9. Genove G, DeMarco U, Xu H, Goins WF, Ahrens ET. A new transgene reporter for in vivo magnetic resonance imaging. Nature Med. 2005; 11(4):450–454. [PubMed: 15778721]
10. Theil EC. Ferritin: structure, gene regulation, and cellular function in animals, plants, and microorganisms. Ann Rev Biochem. 1987; 56:289–315. [PubMed: 3304136]
11. Crichton RR, Wilmet S, Legssyer R, Ward RJ. Molecular and cellular mechanisms of iron homeostasis and toxicity in mammalian cells. J Inorg Biochem. 2002; 91:9–18. [PubMed: 12121757]
12. Arosio P, Levi S. Ferritin, iron homeostasis, and oxidative damage. Free Radical Biol & Med. 2002; 33(4):457–463. [PubMed: 12160928]
13. Deans AE, Wadghiri YZ, Bernas LM, Yu X, Rutt BK, Turnbull DH. Cellular MRI contrast via coexpression of transferrin receptor and ferritin. Magn Reson Med. 2006; 56(1):51–59. [PubMed: 16724301]
14. Liu J, Cheng EC, Long RC Jr, Yang SH, Wang L, Cheng PH, Yang JJ, Wu D, Mao H, Chan AW. Noninvasive Monitoring of Embryonic Stem Cells in vivo with MRI Transgene Reporter. Tissue Eng Part C Methods. Mar 16.2009 Epub ahead of print.
15. Golob JL, Paige SL, Muskheli V, Pabon L, Murry CE. Chromatin remodeling during mouse and human embryonic stem cell differentiation. Dev Dyn. 2008; 237(5):1389–1398. [PubMed: 18425849]
16. Silberstein L, Webster SG, Travis M, Blau HM. Developmental progression of myosin gene expression in cultured muscle cells. Cell. 1986; 46(7):1075–1081. [PubMed: 3530499]
17. Wang, J.; Yarnykh, VL.; Chu, B.; Yuan, C. Improved motion-sensitized driven equilibrium (iMSDE) blood-suppression sequence for atherosclerosis plaque imaging at 3T. 16th Annual Meeting ISMRM; Toronto, Canada. 2008; p. 961Proceedings
18. Leobon B, Garcin I, Menasche P, Vilquin JT, Audinat E, Charpak S. Myoblasts transplanted into rat infracted myocardium are functionally isolated from their host. PNAS. 2003; 100(13):7808–7811. [PubMed: 12805561]
19. Reinecke H, MacDonald GH, Hauschka SD, Murry CE. Electromechanical coupling between skeletal and cardiac muscle. Implications for infarct repair. J Cell Biol. 2000; 149(3):731–740. [PubMed: 10791985]
20. Reinlib L, Field L. Cell transplantation as future therapy for cardiovascular disease? A workshop of the National Heart, Lung, and Blood Institute. Circulation. 2000; 101:E182–187. [PubMed: 10801766]
21. Robey TE, Murry CE. Absence of regeneration in the MRL/MpJ mouse heart following infarction or cryoinjury. Cardiovasc Pathol. 2008; 17(1):6–13. [PubMed: 18160055]
22. van Laake LW, Passier R, Doevendans PA, Mummery CL. Human Embryonic Stem Cell–Derived Cardiomyocytes and Cardiac Repair in Rodents. Circ Res. 2008; 102:1008–1010. [PubMed: 18436793]
23. Robey TE, Saiget MK, Reinecke H, Murry CE. Systems approaches to preventing transplanted cell death in cardiac repair. J Mol Cell Cardiol. 2008; 45(4):567–581. [PubMed: 18466917]
24. Laflamme MA, Chen KY, Naumova AV, Muskheli V, Fugate JA, Dupras SK, Reinecke H, Xu C, Hassanipour M, Police S, O'Sullivan C, Collins L, Chen Y, Minami E, Gill EA, Ueno S, Yuan C, Gold J, Murry CE. Delivery of Human Embryonic Stem Cell Cardiomyocytes in Pro-Survival Factors Enhances the Function of Infarcted Hearts. Nat Biotech. 2007; 25:1015–1024.

25. Cao F, Lin S, Xie X, Ray P, Patel M, Zhang X, Drukker M, Dylla SJ, Connolly AJ, Chen X, Weissman IL, Gambhir SS, Wu JC. In vivo visualization of embryonic stem cell survival, proliferation, and migration after cardiac delivery. Circulation. 2006; 113:1005–1014. [PubMed: 16476845]

26. Meyer N, Jaconi M, Landopoulou A, Fort P, Puceat M. A fluorescent reporter gene as a marker for ventricular specification in ES-derived cardiac cells. FEBS Lett. 2000; 478:151–158. [PubMed: 10922488]

27. Cozzi A, Corsi B, Levi S, Santambrogio P, Albertini A, Arosio P. Overexpression of wild type and mutated human ferritin H-chain in HeLa cells: in vivo role of ferritin ferroxidase activity. J Biol Chem. 2000; 275:25122–25129. [PubMed: 10833524]

28. Papanikolaou G, Pantopoulos K. Iron metabolism and toxicity. Toxicol Appl Pharmacol. 2005; 202:199–211. [PubMed: 15629195]

29. Gossuin Y, Muller RN, Gillis P. Relaxation induced by ferritin: a better understanding for an improved MRI iron quantification. NMR Biomed. 2004; 17(7):427–432. [PubMed: 15526352]

30. Zurkiya O, Chan A, Hu X. Gene based production of magnetic nanoparticles for MRI. Magn Reson Med. 2008; 59(6):1225–1231. [PubMed: 18506784]

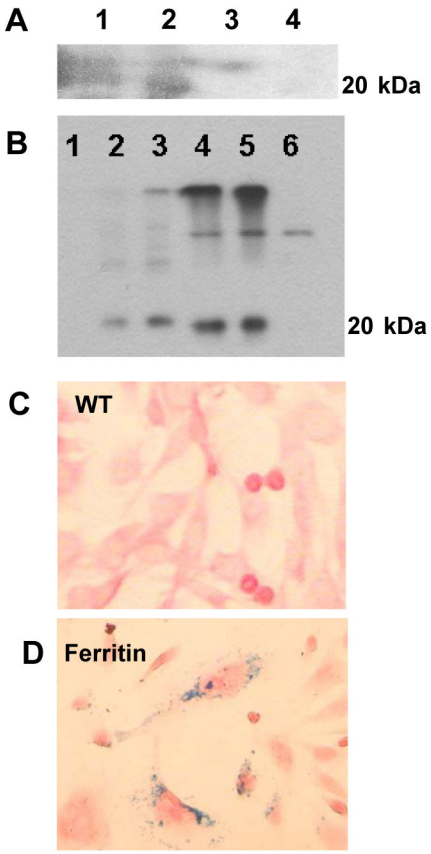

Figure 1. Confirmation of ferritin overexpression in C2C12 cells

A: Western Blot analysis with mouse monoclonal HA-antibody indicating ferritin expression in sense clones (1 and 2) of C2C12 cells transduced by pcDNA3-HAFerr plasmids, but not in antisense clones (3 and 4).

B: Western Blot analysis using monoclonal rabbit antibody to ferritin.

1: Molecular weight ladder.

2: Jurkat cell lysate (ferritin control)

3: SH-SY5Y cell lysate (ferritin control)

4: Transduced C2C12 overexpressing ferritin, mass culture

5: Transduced C2C12 overexpressing ferritin, subclone

6: C2C12 WT (negative control)

C: Prussian Blue staining indicates iron accumulation in C2C12 cells transduced by pcDNA3- HAFerr plasmids, but not in WT cells. To facilitate iron loading cell media in all wells was supplemented with 1mM ferric citrate.

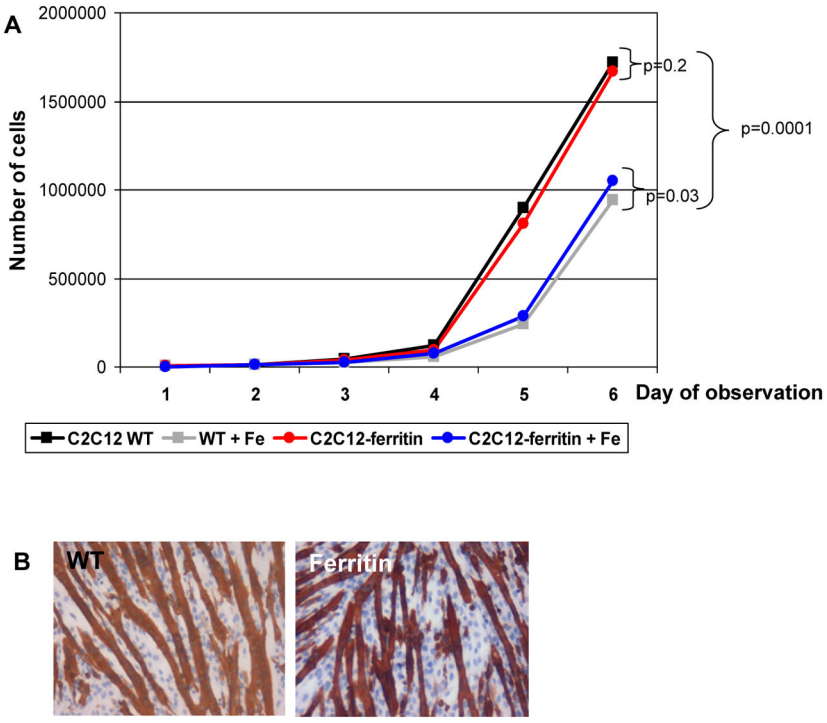

Figure 2. Similar proliferation rate (A) and differentiation pattern (B) of wild type (WT) and transgenic C2C12 overexpressing ferritin

(A) Cell proliferation was assessed by monitoring the total number of cells plated in 6-well plates (5,000 cells per well) during 6 days of growth using a Beckman Coulter Counter. (B) Skeletal myosin heavy chain immunostaining indicated comparable differentiation pattern into multinucleated myotubes in wild type and in transgenic C2C12 cells overexpressing ferritin.

Fe – supplementation of cell media by ferric citrate (1mM).

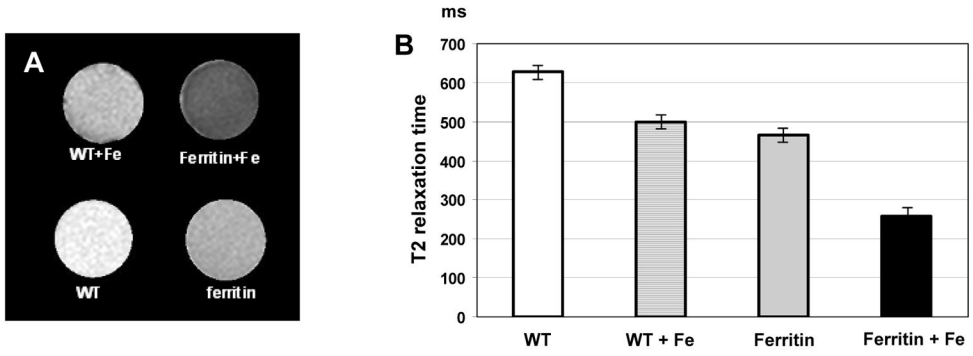

Figure 3. ***In vitro*** **MRI of wild type (WT) and transgenic C2C12 overexpressing ferritin**

A: Transverse relaxation (T2) map of WT cells and C2C12 transduced by pcDNA3-HAferritin construct with and without iron supplementation (Fe:1 mM).

B: Quantification of changes in T2 relaxation time of WT C2C12 and cells transduced by pcDNA3-HAFerritin with and without iron citrate supplementation. Error bars indicate standard deviation of T2 within region of interest on the parametric map.

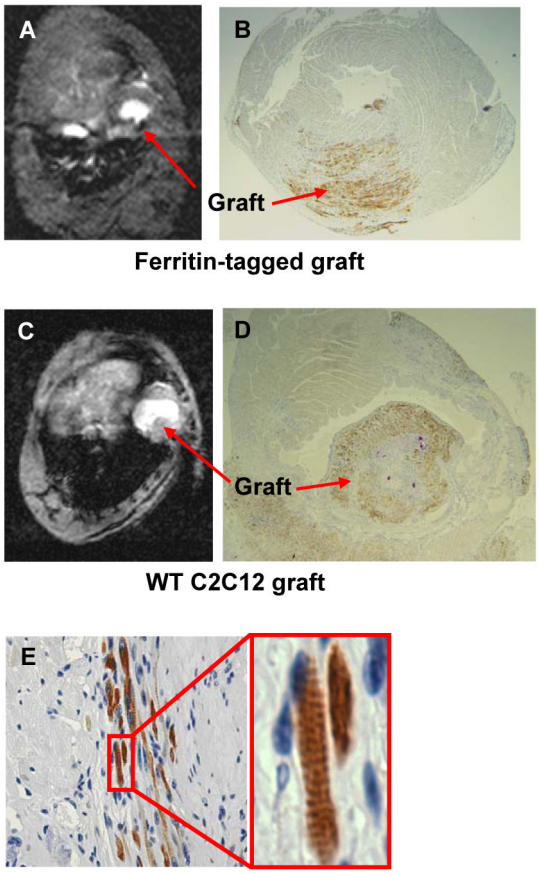

Figure 4. Detection of the skeletal muscle graft in the infarcted mouse heart

C2C12 cells were not incubated with iron supplement prior to transplantation.

A, B: Graft detection *in vivo* by MRI and *ex vivo* by embryonic myosin staining 3 weeks after transplantation of 500,000 transgenic C2C12 cells overexpressing ferritin. Stable signal void is revealed in the left ventricle indicating presence of transgenic graft.

C, D: *In vivo* MRI and histology of the mouse heart 3 weeks after engraftment of 500,000 wild-type C2C12 cells. Large skeletal muscle graft is well defined as non-contracting invagination into left ventricle chamber of the heart. No signal void is detected by T2* sequence in the area of wild-type graft.

E: Embryonic skeletal myosin heavy chain staining of the mouse heart reveals presence of the skeletal muscle graft. Graft cells are well differentiated and contain sarcomeres.

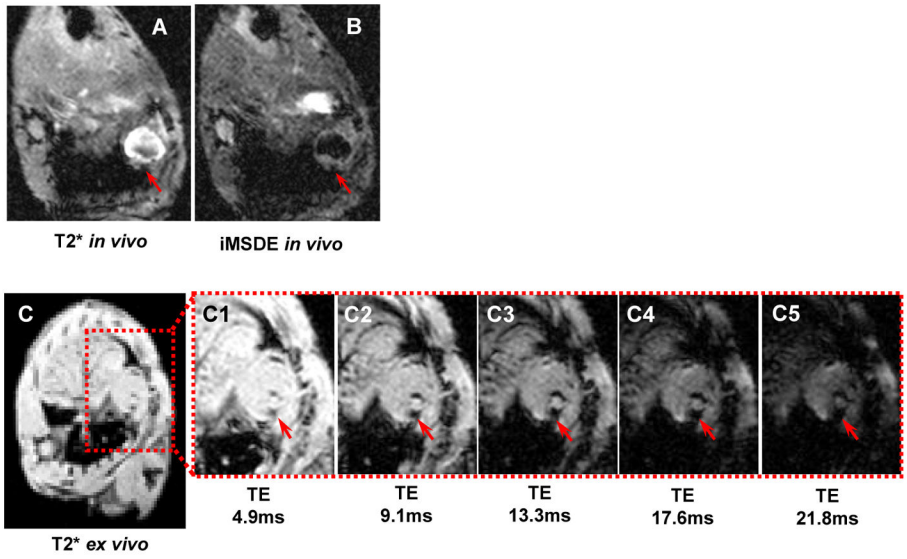

Figure 5. Reproducibility of detection of transgenic ferritin-overexpressing grafts in the infarcted mouse heart

A: *In vivo* T2*-weighted bright-blood turbo gradient echo cine sequence, TR=15ms; TE=9.3ms; flip angle 15°; slice thickness 0.8 mm; acquisition voxel size 0.25/0.25mm, reconstruction voxel size 0.10/0.10mm; 6 signal averages.

B: *In vivo* 2D iMSDE-prepared (improved motion sensitized driven equilibrium) black blood turbo spin-echo pulse sequence: TR=16ms; TE=9.8ms; flip angle 15°; slice thickness 0.8mm; acquisition voxel size 0.26/0.26mm, reconstruction voxel size 0.10/0.10 mm; 10 signal averages.

C: *Ex vivo* detection of the graft on post-mortem images (10 min after euthanasia) using multiple gradient echoes. Increase of the echo time (TE) makes MR images more T2*-weighted and thus makes a cellular graft better visible in the mouse heart (arrow). Sequence parameters: 3D gradient echo, TR 61.8ms; FA 10°; slice thickness 0.5mm; acquisition matrix 248x248; 2 signal averages.

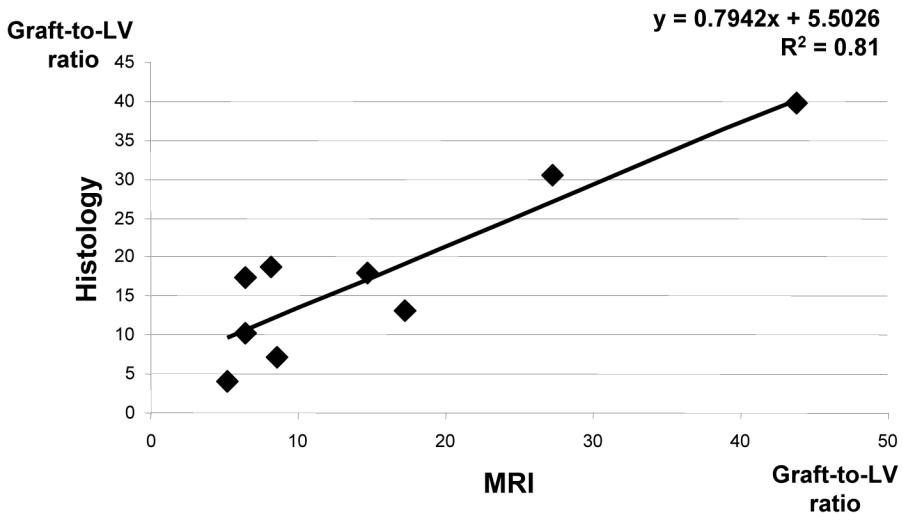

Figure 6. Correlation between MRI and histological measurements of graft size

There was a good agreement between the two techniques, with the regression line not significantly different from the line of unity.